Journal of Colloid and Interface Science **233,** 259–264 (2001)
doi:10.1006/jcis.2000.7223, available online at http://www.idealibrary.com on IDEAL®

# Modeling Competitive Adsorption of Molybdate, Sulfate, and Selenate on $\gamma$-$Al_2O_3$ by the Triple-Layer Model

Chung-Hsin Wu,* Shang-Lien Lo,* Cheng-Fang Lin,* and Chao-Yin Kuo†,[1]

*Graduate Institute of Environmental Engineering, National Taiwan University, 71 Chou-Shan Road, Taipei, 106, Taiwan; and †Institute and Department of Labor Relations, Chinese Culture University, 55 Hwa Kong Road, Shih-Lin District, Taipei, Taiwan

Received June 5, 2000; accepted September 11, 2000

**Competitive adsorption of molybdate, sulfate, and selenate onto $\gamma$-$Al_2O_3$ was investigated in the present study. Binary solute systems of $MoO_4^{2-} + SO_4^{2-}$, $MoO_4^{2-} + SeO_4^{2-}$, and $SO_4^{2-} + SeO_4^{2-}$ and a ternary solute system of $MoO_4^{2-} + SO_4^{2-} + SeO_4^{2-}$ were evaluated to determine their relative effects on competitive adsorption on the $\gamma$-$Al_2O_3$ surface. Anionic competitive adsorption efficiency was pH dependent. The higher the pH, the lower the efficiency of $MoO_4^{2-}$ in preventing $SO_4^{2-}$ and $SeO_4^{2-}$ adsorption; similar results were found in $SeO_4^{2-}$ depressing $SO_4^{2-}$ adsorption. This research found that more sites are occupied in mixed anionic adsorbate systems than when either ion is present alone. The results suggest that the $\gamma$-$Al_2O_3$ surface is composed of many groups of binding sites. Because of the heterogeneity of adsorption sites, the triple-layer model (TLM) predicted the competitive effects qualitatively but not quantitatively. TLM gave reasonable descriptions of molybdate adsorption in the presence of sulfate and selenate, indicating that the model may be useful in predicting molybdate adsorption on $\gamma$-$Al_2O_3$.** 

*Key Words:* **competitive adsorption; molybdate; sulfate; selenate; triple-layer model.**

## INTRODUCTION

Molybdenum is an essential trace element for protein synthesis and oxidation in human metabolism (1). Like other transition metals, molybdenum and/or molybdate compounds are toxic to grazing animals as well as humans (2); the degree of toxicity of molybdenum and/or molybdate compounds ranks between those of Zn(II) and Cr(III) compounds. Selenate is a major selenium species in drainage water (3) and sulfate is the most abundant anion in atmospheric deposition. The presence of these anions in wastewater and surface water is becoming a severe environmental and public health problem.

The adsorption of molybdate, sulfate, and selenate has been extensively studied. Zhang and Sparks (4–6) have studied the kinetics of molybdate, sulfate, and selenate on goethite by the pressure-jump technique. Wu *et al.* (7, 8) investigated the kinetics and mechanisms of molybdate, sulfate, and selenate adsorption/desorption at the $\gamma$-$Al_2O_3$/water interface. Roy *et al.* (9) indicate that the adsorption of arsenate and molybdate was significantly reduced by the competitive adsorption of phosphate. Manning and Goldberg (10) showed that molybdate decreased As(V) adsorption only below pH 6. They also (11) explored the presence of molybdate at equimolar and 10 times greater concentration than As(V) and found that there were only slight decreases in As(V) adsorption. Sulfate decreased the adsorption of As(III), As(V), and phosphate, but sulfate adsorption increased with increasing adsorption of $Ca^{2+}$ (12–14). Goldberg *et al.* (15) showed that the competitive anion effects on B adsorption increased in the order sulfate < molybdate < phosphate. In most of the previous studies, the influence of competitive adsorption on anion partitioning has been addressed in binary solute systems containing a strongly binding anion with an organic compound or sulfate (16). A systematic investigation on the relative competition for sorption onto oxides among various anions with different binding affinities is rather limited. In practice, multicomponent competition might increase the complexity of anion interactions at the water/oxide interfaces. Such complex systems frequently occur, and the magnitude of these competitive interactions needs to be clarified in order to better predict contaminant behavior and to identify anions that are more likely to be affected in their transport in the presence of other anions.

The study discussed here is an extension of the kinetic studies on molybdate, sulfate, and selenate on $\gamma$-$Al_2O_3$ and our previous paper (7, 8, 17) on the competitive adsorption systems of molybdate, sulfate, and selenate. The objectives of this study were to (i) determine the extent of competitive adsorption between molybdate, sulfate, and selenate on $\gamma$-$Al_2O_3$ as a function of pH and (ii) ascertain the accuracy of the triple-layer model (TLM) in predicting adsorption in competitive adsorption systems for a wide range of pH values.

## MATERIALS AND METHODS

### *Materials*

Stock anion solutions ($2.5 \times 10^{-2}$ M) were prepared with $Na_2MoO_4$, $Na_2SO_4$ and $Na_2SeO_4$(reagent grade from Merck)

[1] To whom correspondence should be addressed. Fax: +886-2-22398355. E-mail: kuocyr@ms35.hinet.net.



0021-9797/01 $35.00

and distilled/deionized water (Milli-Q SP). $\gamma$-$Al_2O_3$ (Aerosil Co., Japan) was purified by electrodialysis (1200 V, 3 mA) before use to remove impure substances which could affect adsorption results. The surface area of $\gamma$-$Al_2O_3$, determined by the $N_2$ Brunauer–Emmett–Teller sorption experiments, was equal to 100 $m^2/g$.

In the competitive adsorption experiments, anions ($5 \times 10^{-3}$ M) were equilibrated with $\gamma$-$Al_2O_3$ suspension (30 g/l), and the pH of the suspension was adjusted with a small amount of $HNO_3$ or NaOH to cover pH 2–10 for $MoO_4^{2-} + SO_4^{2-}$, pH 2–9 for $MoO_4^{2-} + SeO_4^{2-}$ and $SO_4^{2-} + SeO_4^{2-}$, and pH 4–9 for $MoO_4^{2-} + SO_4^{2-} + SeO_4^{2-}$. These pH values were chosen for understanding the relative binding strength between anions. After the desired pH was reached, 10 ml of the suspension was extracted to a 15-ml polypropylene tube. All experiments were performed in a tightly capped 15-ml polypropylene tube under $N_2$ atmosphere at $25 \pm 0.1$°C for 24 h. At the end of the equilibrium period, the pH of each suspension was determined. The suspensions were centrifuged at 9500 rpm for 10 min, and the supernatant was then filtered through 0.2-$\mu$m filter paper (Gelman Sciences). All anion concentrations were determined by ion chromatography (Dionex 2000i SP).

*Modeling of Competitive Adsorption Data*

The TLM developed by Davis and Leckie (18) and subsequently modified by Hayes and Leckie (19) was used to simulate the equilibrium partitioning of anion species at the $\gamma$-$Al_2O_3$/water interface. The modified TLM differs from the original model in two ways. First, the adsorbed ion can be located on both the o-layer and $\beta$-layer; i.e., ions are allowed to form either inner- or outer-sphere surface complexes. Second, the chemical potential and standard and reference states are defined equivalently for both solution and surface species, leading to a different relationship between the activity coefficients and the interfacial potential than previously used. The TLM parameters and intrinsic acidity surface hydrolysis constant ($K_{a1}^{int}$ and $K_{a2}^{int}$) and binding constants ($K_{Na^+}^{int}$ and $K_{NO_3^-}^{int}$) of the background electrolyte ($NaNO_3$) with the surface are described in Table 1. Potentiometric titration experiments on 10 g/l $\gamma$-$Al_2O_3$ suspensions with three different background electrolyte concentrations (0.1, 0.01, and 0.001 N) to calculate $K_{a1}^{int}$ and $K_{a2}^{int}$ and $K_{Na^+}^{int}$ and $K_{NO_3^-}^{int}$ follow the method of Davis *et al.* (22). The acidity constants were determined by extrapolating the titration data at the lowest $NaNO_3$ concentration to zero fractional ionization. Similarly, the electrolyte binding constants were estimated by extrapolating the higher $NaNO_3$ concentration results to zero fractional ionization. The $\log K_{a1}^{int}$, $\log K_{a2}^{int}$, $\log K_{Na^+}^{int}$, and $\log K_{NO_3^-}^{int}$ values determined in this work were −6.9, −9.7, −8.3, and 6.9, respectively. For comparison, the $\log K_{a1}^{int}$ and $\log K_{a2}^{int}$ values reported by Hohl and Stumm (23) were −7.2 and −9.5. The $\log K_{Na^+}^{int}$ and $\log K_{NO_3^-}^{int}$ values reported by Zhang and Sparks (5) and Hayes and Leckie (19) were −9.1 and 8.7. The equations for TLM simulation are presented below:

**TABLE 1**
**TLM Parameters and Basic Surface Complexation Constants**

| | |
|---|---|
| Specific surface area ($m^2/g$) | 100 (BET measurement) |
| Site density (site/$nm^2$) | 8 (20) |
| $C_1$ (o-plane capacitance, $\mu F/cm^2$) | 80 (21) |
| $C_2$ ($\beta$-plane capacitance, $\mu F/cm^2$) | 20 (21) |
| $\log K_{a1}^{int}$, $\log K_{a2}^{int}$ | −6.9, −9.7 (acid/base titration) |
| $\log K_{Na^+}^{int}$, $\log K_{NO_3^-}^{int}$ | −8.3, 6.9 (acid/base titration) |

$$SOH_2^+ \rightleftharpoons SOH + H^+, \quad [1]$$

$$SOH \rightleftharpoons SO^- + H^+, \quad [2]$$

$$SOH + Na^+ \rightleftharpoons SO^- - Na^+ + H^+, \quad [3]$$

$$SOH + H^+ + NO_3^- \rightleftharpoons SOH_2^+ - NO_3^-, \quad [4]$$

$$SOH + H^+ + L^{2-} \rightleftharpoons SOH_2^+ - L^{2-}, \quad [5]$$

$$SOH + H^+ + L^{2-} \rightleftharpoons SL^- + H_2O. \quad [6]$$

Equations [1] and [2] describe protonation of reacting surface sites, and Eqs. [3] and [4] describe the formation of complexes between the background electrolyte ions and the surface. Ion pairs are formed at the $\beta$-plane (Eq. [5]), where the adsorption is nonspecific and the reaction product is an outer-sphere surface complex, if $L^{2-}$ ($L^{2-}$ denotes $MoO_4^{2-}$, $SO_4^{2-}$, or $SeO_4^{2-}$) reacts similarly to a background electrolyte with SOH. If adsorption of $L^{2-}$ is visualized as a chemically specific reaction, the reaction, however, can be expressed as an inner-sphere surface coordination process (Eq. [6]). Equation [6] represents the reaction of $L^{2-}$ with 1 mol of reactive surface hydroxyl to form an inner-sphere monodentate surface complex.

The intrinsic conditional equilibrium constants for the previous reactions can be defined as

$$K_{a1}^{int} = \frac{[SOH][H^+]}{[SOH_2^+]} \exp\left(\frac{-\varphi_o F}{RT}\right) \quad [7]$$

$$K_{a2}^{int} = \frac{[SO^-][H^+]}{[SOH]} \exp\left(\frac{-\varphi_o F}{RT}\right) \quad [8]$$

$$K_{Na^+}^{int} = \frac{[SO^- - Na^+][H^+]}{[SOH][Na^+]} \exp\left[\frac{(\varphi_\beta - \varphi_o)F}{RT}\right] \quad [9]$$

$$K_{NO_3^-}^{int} = \frac{[SOH_2^+ - NO_3^-]}{[SOH][H^+][NO_3^-]} \exp\left[\frac{(\varphi_o - \varphi_\beta)F}{RT}\right] \quad [10]$$

$$K_{L_{out}^{2-}}^{int} = \frac{[SOH_2^+ - L^{2-}]}{[SOH][H^+][L^{2-}]} \exp\left[\frac{(\varphi_o - 2\varphi_\beta)F}{RT}\right] \quad [11]$$

$$K_{L_{in}^{2-}}^{int} = \frac{[SL^-]}{[SOH][H^+][L^{2-}]} \exp\left(\frac{-\varphi_o F}{RT}\right), \quad [12]$$

where $F$ is the Faraday constant, $R$ is the universal gas constant, $T$ is the absolute temperature, and $\varphi_o$ and $\varphi_\beta$ are the electrical potentials at the o- and $\beta$-plane, respectively. The equilibrium and mass balance equations are solved simultaneously in

**TABLE 2**
**Intrinsic Rate Constants and Equilibrium Constants of Anions**

| | $k_1^{int}$, $M^{-2}$ $s^{-1}$ | $k_{-1}^{int}$, $s^{-1}$ | $k_2^{int}$, $s^{-1}$ | $k_{-2}^{int}$, $s^{-1}$ | log $K_{eq}^{int}$ | $n$ |
|---|---|---|---|---|---|---|
| $MoO_4^{2-}$ | $5.2 \times 10^{6}$ [a] | $2.4 \times 10^{1}$ [a] | 1.7[a] | $3.6 \times 10^{-1}$ [a] | 6.5[b] | 0.68[b] |
| $SO_4^{2-}$ | $2.7 \times 10^{8}$ [c] | $1.1 \times 10^{-2}$ [c] | — | — | 10.4[b] | 0.17[b] |
| $SeO_4^{2-}$ | $4.3 \times 10^{8}$ [c] | $4.4 \times 10^{-2}$ [c] | — | — | 9.8[b] | 0.22[b] |

[a] Wu *et al.* (7).
[b] Wu *et al.* (17).
[c] Wu *et al.* (8).

the TLM. Data were modeled with the TLM by assuming that (i) homogeneous sites and (ii) the intrinsic surface complexation constants obtained for the adsorption of molybdate, sulfate, and selenate from a single anion system can be used to predict simultaneously, competitive adsorption from mixtures of two of the anions.

The parameters in Tables 1 and 2 and Eqs. [1]–[12] were used in the model analysis to determine the anion partition for the competitive adsorption systems.

## RESULTS AND DISCUSSIONS

### *Competitive Adsorption Envelope*

Anionic adsorbates directly compete for available binding sites and indirectly interact through alteration of the electrostatic charge at the solid surface. Both interactions are influenced by solution pH and intrinsic binding affinities of the adsorbates.

Figure 1 shows the influence of pH on the competitive adsorption of $MoO_4^{2-}$ and $SO_4^{2-}$ by $\gamma$-$Al_2O_3$. The adsorption of $MoO_4^{2-}$ is not influenced by $SO_4^{2-}$. On the contrary, the adsorption of $SO_4^{2-}$ is inhibited by $MoO_4^{2-}$ significantly. Wu *et al.* (7, 8) explored the phenomena of molybdate forming an inner-sphere complex and sulfate forming an outer-sphere complex on $\gamma$-$Al_2O_3$. Since the inner-sphere anion is a stronger adsorbate

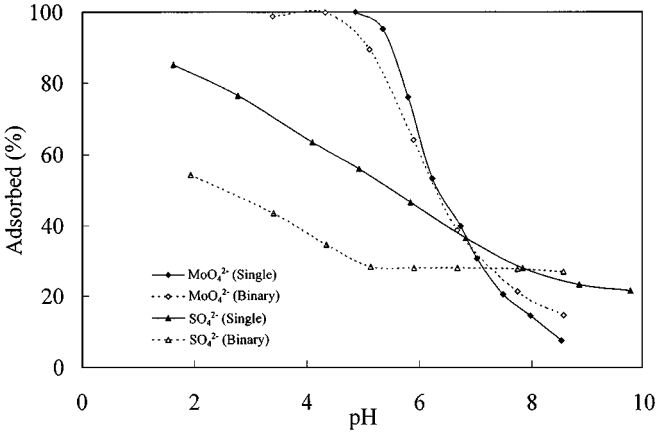


**FIG. 1.** Competitive adsorption of molybdate and sulfate on $\gamma$-$Al_2O_3$ as a function of pH ($\gamma$-$Al_2O_3$ = 30 g/l, $[MoO_4^{2-}] = [SO_4^{2-}] = 5 \times 10^{-3}$ M).

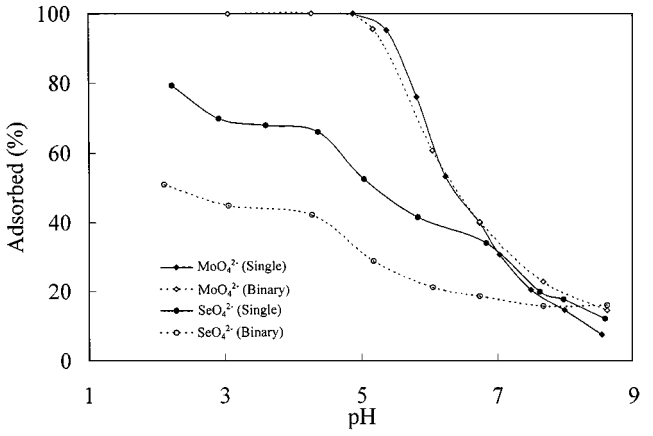


**FIG. 2.** Competitive adsorption of molybdate and selenate on $\gamma$-$Al_2O_3$ as a function of pH ($\gamma$-$Al_2O_3$ = 30 g/l, $[MoO_4^{2-}] = [SeO_4^{2-}] = 5 \times 10^{-3}$ M).

than the outer-sphere anion, the finding of Fig. 1 is reasonable. Goldberg *et al.* (15) displayed the order of anion adsorption by soil to be molybdate > sulfate. Our results on anionic competitive adsorption—molybdate > sulfate—are in agreement with this finding.

The experimental $MoO_4^{2-}$ and $SO_4^{2-}$ adsorption envelopes on $\gamma$-$Al_2O_3$ in the binary system also suggest that $MoO_4^{2-}$ and $SO_4^{2-}$ compete for adsorption sites on the $\gamma$-$Al_2O_3$ surface. It is interesting to note that, in the absence of $MoO_4^{2-}$, the quantities of $SO_4^{2-}$ adsorbed on $\gamma$-$Al_2O_3$ surfaces significantly decreased with increasing pH, but, in the presence of $MoO_4^{2-}$, $SO_4^{2-}$ adsorption was less influenced by pH, particularly at pH > 5. The explanation may be due to a change in the $\gamma$-$Al_2O_3$ surface charge caused by the concomitant.

Shown in Fig. 2 are the differences between single adsorbate and binary adsorbate systems when $MoO_4^{2-}$ and $SeO_4^{2-}$ are adsorbed as a function of pH. The binary anion systems of $MoO_4^{2-}/SO_4^{2-}$ and $MoO_4^{2-}/SeO_4^{2-}$ exhibit similar results on competitive adsorption. Molybdate adsorption is insignificantly restrained in the presence of sulfate or selenate. On the other hand, sulfate and selenate adsorption are significantly influenced in the presence of molybdate at acidic pH, where a 30% decrease in adsorption is noticed. Molybdate adsorption on $\gamma$-$Al_2O_3$ displayed a stronger pH dependence in single anion and binary anion systems than sulfate or selenate, with 10% $MoO_4^{2-}$ adsorption above pH 8 and a steep adsorption edge resulting in 100% $MoO_4^{2-}$ adsorption below pH 5. Molybdate competitive adsorption caused a shift in the sulfate and selenate adsorption edge ($pH_{50}$) from pH 5.6 to 2.4 in the $MoO_4^{2-}/SO_4^{2-}$ system and from pH 5.2 to 2.2 in the $MoO_4^{2-}/SeO_4^{2-}$ system, but it did not change the overall shape of the $SeO_4^{2-}$ adsorption envelope.

Results of sulfate and selenate competitive adsorption experiments as a function of pH are presented in Fig. 3. It is interesting to note that, when sulfate and selenate were added alone, more sulfate than selenate was adsorbed in the range of pH 2 to 9. In contrast, when sulfate and selenate ions were added as a mixture ($SO_4^{2-} + SeO_4^{2-}$), more selenate than sulfate was adsorbed on the

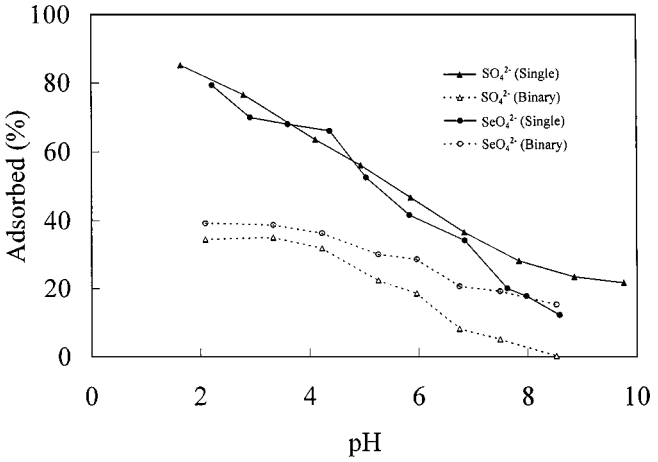


**FIG. 3.** Competitive adsorption of sulfate and selenate on $\gamma$-$Al_2O_3$ as a function of pH ($\gamma$-$Al_2O_3$ = 30 g/l, $[SO_4^{2-}] = [SeO_4^{2-}] = 5 \times 10^{-3}$ M).

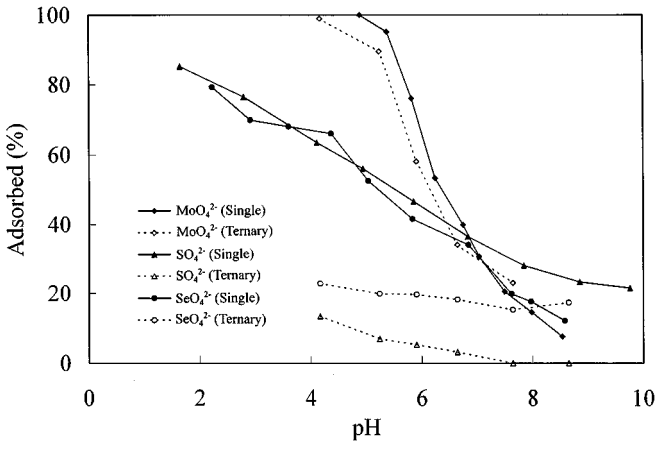


**FIG. 4.** Competitive adsorption of molybdate, sulfate, and selenate on $\gamma$-$Al_2O_3$ as a function of pH ($\gamma$-$Al_2O_3$ = 30 g/l, $[MoO_4^{2-}] = [SO_4^{2-}] = [SeO_4^{2-}] = 5 \times 10^{-3}$ M).

surface of $\gamma$-$Al_2O_3$ in the range of pH studied. The reason for this may be that the sites on the $\gamma$-$Al_2O_3$ surface have a stronger affinity for selenate than for sulfate. Competition between two anions for a given surface site depends on the strength and type of binding between the anion and the surface and on the binding rate on the surface.

The intrinsic rate constants and equilibrium constants of molybdate, sulfate, and selenate are shown in Table 2. The intrinsic desorption rate constants ($k_{-1}^{\text{int}}$) were far smaller than the intrinsic adsorption rate constants ($k_1^{\text{int}}$) for sulfate and selenate. Therefore, the binding rate on the surface may control the competitive adsorption results. The $k_1^{\text{int}}$ of selenate ($4.3 \times 10^8$ $M^{-2}$ $s^{-1}$) is larger than that of sulfate ($2.7 \times 10^8$ $M^{-2}$ $s^{-1}$), and it is suggested that the affinity for the $\gamma$-$Al_2O_3$ surface of selenate is larger than that of sulfate. This suggestion agrees with the experimental results.

Anion competitive adsorption efficiency was pH dependent. The higher the pH, the lower the efficiency of $MoO_4^{2-}$ in preventing $SO_4^{2-}$ and $SeO_4^{2-}$ adsorption; similar results were found in $SeO_4^{2-}$ depressing $SO_4^{2-}$ adsorption. In the range of pH 4 to 7, the efficiency of $MoO_4^{2-}$ decreased from 26% to 8% in the $MoO_4^{2-} + SO_4^{2-}$ system and from 23% to 13% in the $MoO_4^{2-} + SeO_4^{2-}$ system, and the efficiency of $SeO_4^{2-}$ decreased from 32% to 28% in the $SO_4^{2-} + SeO_4^{2-}$ system. The results of Figs. 1–3 show that the combined amounts of $MoO_4^{2-}$ and $SO_4^{2-}$ adsorbed in the $MoO_4^{2-} + SO_4^{2-}$ system, $MoO_4^{2-}$ and $SeO_4^{2-}$ adsorbed in $MoO_4^{2-} + SeO_4^{2-}$ system, and $SO_4^{2-}$ and $SeO_4^{2-}$ adsorbed in $SO_4^{2-} + SeO_4^{2-}$ systems were usually higher than that of $MoO_4^{2-}$, $SO_4^{2-}$, or $SeO_4^{2-}$ adsorbed when added alone; evidently, some sites are specific to one anion. Similar results were inferred by Hingston *et al.* (24) and Violante *et al.* (25), who found that, in mixed phosphate plus arsenate or phosphate plus selenite or phosphate plus oxalate systems, it is possible to occupy more sites with anions than when either ion is present alone.

Figure 4 shows the competitive adsorption for mixtures of $MoO_4^{2-}$, $SO_4^{2-}$, and $SeO_4^{2-}$. The results agree with those of Figs. 1–3: $MoO_4^{2-}$ inhibits the adsorption of $SO_4^{2-}$ and $SeO_4^{2-}$, and $SeO_4^{2-}$ inhibits the adsorption of $SO_4^{2-}$. Table 2 presents the order of overall proton coefficients ($n$) as $MoO_4^{2-} > SeO_4^{2-} > SO_4^{2-}$, which fits the adsorption affinity between $MoO_4^{2-}$, $SO_4^{2-}$, and $SeO_4^{2-}$, as shown in Figs. 1–4. Wu *et al.* (17) suggested that a larger value of the overall proton coefficient corresponds to a higher affinity for the oxide surface. This research found the relative retention of anions on $\gamma$-$Al_2O_3$ surface to be molybdate > selenate > sulfate, which agrees with the findings of Wu *et al.* (17).

### *TLM Modeling of Competitive Adsorption*

The experimental data of Figs. 1–4 were simulated by the TLM model and are presented in Figs. 5–8. In the simulation for anion competition, all parameters were maintained at the same values as in the single anion systems (Tables 1 and 2). Figures 5 and 6 show the TLM simulation in $MoO_4^{2-} + SO_4^{2-}$

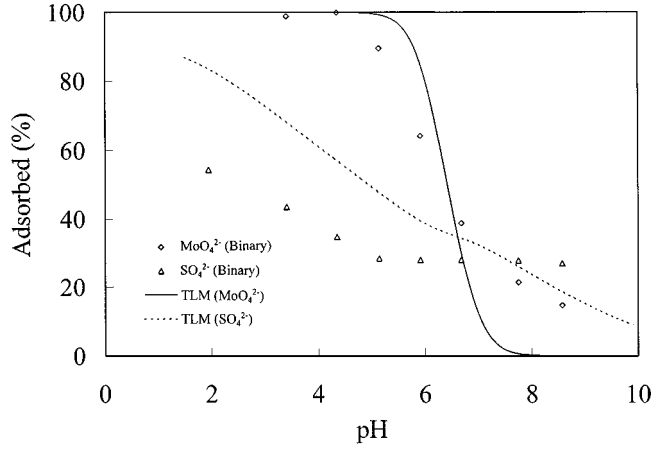


**FIG. 5.** Binary solute adsorption of molybdate and sulfate on $\gamma$-$Al_2O_3$ as a function of pH. TLM simulations are shown with lines and symbols denote experimental data.

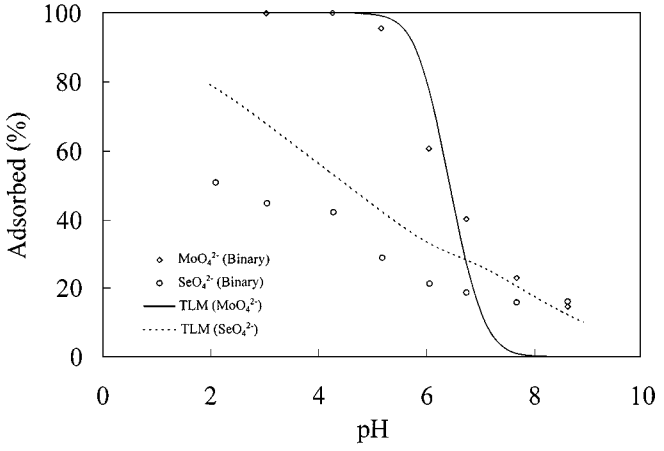


**FIG. 6.** Binary solute adsorption of molybdate and selenate on $\gamma$-$Al_2O_3$ as a function of pH. TLM simulations are shown with lines and symbols denote experimental data.

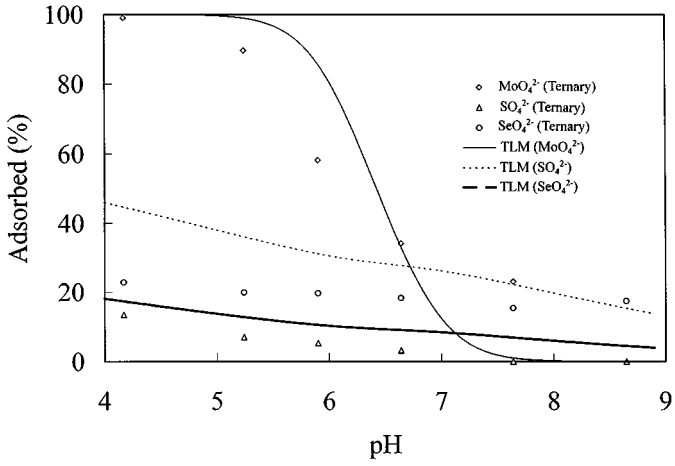


**FIG. 8.** Ternary solute adsorption of molybdate, sulfate, and selenate on $\gamma$-$Al_2O_3$ as a function of pH. TLM simulations are shown with lines and symbols denote experimental data.

and $MoO_4^{2-} + SeO_4^{2-}$ systems, respectively. The simulation results of $MoO_4^{2-}$ in binary adsorbate systems were nearly the same as in single adsorbate systems reported by Wu *et al.* (17). In contrast, results for $SO_4^{2-}$ and $SeO_4^{2-}$ were significantly overpredicted. The TLM may represent mixed molybdate–sulfate and molybdate–selenate anion systems qualitatively only, but it does reproduce the shape of adsorption envelopes over the entire pH range studied.

Figure 7 displays the TLM simulation results of the $SO_4^{2-} + SeO_4^{2-}$ system. Experimental data showed that $SeO_4^{2-}$ inhibited $SO_4^{2-}$ adsorption on a $\gamma$-$Al_2O_3$ surface, but the simulation results presented a contradictory trend. Benjamin and Leckie (26) indicated that measured adsorption equilibrium constants were often average values for adsorption reactions involving several different site types. As a result, the assumption that surface sites are available in excess may be invalid for some site types even though the overall surface coverage is far from saturation. The TLM is based on the assumption that adsorption occurs on only one type of site. While this assumption has been adequate for the modeling of single anion systems, this study indicates that it is very likely an oversimplification. Oxide surfaces contain features such as steps and irregularly broken edges that will contribute to site heterogeneity and, thus, specific binding energies at different surface sites. Several researchers have found evidence for site heterogeneity on oxide surfaces (10, 11, 25–28). Therefore, the misjudgment of TLM simulation in $SO_4^{2-} + SeO_4^{2-}$ competitive adsorption systems may be attributed to the site heterogeneity on $\gamma$-$Al_2O_3$ surfaces.

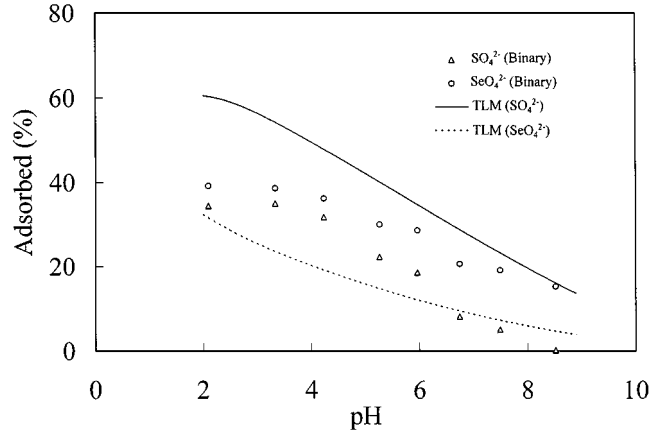


**FIG. 7.** Binary solute adsorption of sulfate and selenate on $\gamma$-$Al_2O_3$ as a function of pH. TLM simulations are shown with lines and symbols denote experimental data.

Figure 8 shows the results of the TLM simulation of ternary solute ($MoO_4^{2-} + SO_4^{2-} + SeO_4^{2-}$) systems. As observed in Figs. 5 and 6 for molybdate, the shape of the competitive adsorption envelope predicted by TLM is similar to that of the experimental adsorption envelope. For sulfate and selenate, the mistaken prediction is due to site heterogeneity. Since the TLM is capable of producing the shape of anion adsorption envelopes from mixed solutions qualitatively, it appears likely that TLM is an appropriate representation of anionic competition. However, quantitative verification of the model's ability to describe anionic competition using a single set of reactive sites will not be possible without improvements in certain model parameters.

## CONCLUSIONS

Competitive adsorption of anions affects the partitioning and transport of anionic solutes in subsurface and surface water. The competitive adsorption results show that the anions which form inner-sphere complexes inhibit the outer-sphere complexes formed. For anions with the same adsorption mechanisms, this study suggests that the larger the binding rate on the oxide surface, the greater the affinity on oxide surface. The TLM adequately describes experimental anionic adsorption envelopes on $\gamma$-$Al_2O_3$ and is useful in providing a modeling framework in which to test assumptions regarding the mechanism of anion

adsorption. For molybdate, the shape of the competitive adsorption envelope predicted by the TLM is similar to that of the experimental adsorption envelope, indicating that the TLM may be useful in predicting molybdate adsorption on $\gamma$-$Al_2O_3$.

## ACKNOWLEDGMENTS

The authors thank the reviewers for their constructive comments. The authors also express their sincere thanks to the National Science Council, Taiwan, R.O.C., for its financial support (Contract Nos. NSC 88-2211-E-002-020 and NSC 89-2211-E-034-004) of this study.

## REFERENCES

1. Parker, G. A., "Analytical Chemical of Molybdenum," Springer-Verlag, Berlin, Germany, 1983.
2. Bodek, I., Lyman, W. J., Reehl, W. F., and Rosenblatt, D. H., "Environmental Inorganic Chemistry," Pergamon Press, New York, 1988.
3. Zhang, Y., and Moore, J. N., *Environ. Sci. Technol.* **30,** 2613–2619 (1996).
4. Zhang, P. C., and Sparks, D. L., *Soil Sci. Soc. Am. J.* **53,** 1028–1034 (1989).
5. Zhang, P. C., and Sparks, D. L., *Soil Sci. Soc. Am. J.* **54,** 1266–1273 (1990).
6. Zhang, P. C., and Sparks, D. L., *Environ. Sci. Technol.* **24,** 1848–1856 (1990).
7. Wu, C. H., Lin, C. F., Lo, S. L., and Yasunaga, T., *J. Colloid Interface Sci.* **208,** 430–438 (1998).
8. Wu, C. H., Lin, C. F., and Lo, S. L., *J. Environ. Sci. Health A* **34,** 605–624 (1999).
9. Roy, W. R., Hassett, J. J., and Griffin, R. A., *Soil Sci. Soc. Am. J.* **50,** 1176–1182 (1986).
10. Manning, B. A., and Goldberg, S., *Soil Sci. Soc. Am. J.* **60,** 121–131 (1996).
11. Manning, B. A., and Goldberg, S., *Clays Clay Miner.* **44,** 609–623 (1996).
12. Bolan, N. S., Syers, J. K., and Sumner, M. E., *Soil Sci. Soc. Am. J.* **57,** 691–696 (1993).
13. Hawke, D., Carpenter, P. D., and Hunter, K. A., *Environ. Sci. Technol.* **23,** 187–191 (1989).
14. Wilkie, J. A., and Hering, J. G., *Colloids Surf. A* **107,** 97–110 (1996).
15. Goldberg, S., Forster, H. S., Lesch, S. M., and Heick, E. L., *Soil Sci.* **161,** 99–103 (1996).
16. Dynes, J. J., and Huang, P. M., *Soil Sci. Soc. Am. J.* **61,** 772–783 (1997).
17. Wu, C. H., Lo, S. L., and Lin, C. F., *Colloids Surf. A* **166,** 251–259 (2000).
18. Davis, J. A., and Leckie, J. O., *J. Colloid Interface Sci.* **74,** 32–43 (1980).
19. Hayes, K. F., and Leckie, J. O., *J. Colloid Interface Sci.* **115,** 564–572 (1987).
20. Peri, J. B., *J. Phys. Chem.* **69,** 211–219 (1965).
21. Hayes, K. F., Radden, G., Ela, W., and Leckie, J. O., *J. Colloid Interface Sci.* **142,** 448–469 (1991).
22. Davis, J. A., James, R. O., and Leckie, J. O., *J. Colloid Interface Sci.* **63,** 480–499 (1978).
23. Hohl, M., and Stumm, W., *J. Colloid Interface Sci.* **55,** 281–288 (1976).
24. Hingston, F. J., Posner, A. M., and Quirk, J. P., *Discuss. Faraday Soc.* **52,** 334–342 (1971).
25. Violante, A., Colombo, C., and Buondonno, A., *Soil Sci. Soc. Am. J.* **55,** 65–70 (1991).
26. Benjamin, M. M., and Leckie, J. O., *J. Colloid Interface Sci.* **79,** 209–221 (1981).
27. Goldberg, S., *Soil Sci. Soc. Am. J.* **49,** 851–856 (1985).
28. Benyahya, L., and Garnier, J. M., *Environ. Sci. Technol.* **33,** 1398–1407 (1999).